VU Research Portal

Modeling regional to global CH4 emissions of boreal and arctic wetlands

Petrescu, A.M.R.; van Beek, L.P.H.; van Huissteden, J.; Prigent, C.; Sachs, T.; Corradi, C.A.R.; Parmentier, F.J.W.; Dolman, A.J.

Link to publication in VU Research Portal

Modeling regional to global CH$_4$ emissions of boreal and arctic wetlands

A. M. R. Petrescu,[1,2] L. P. H. van Beek,[3] J. van Huissteden,[1] C. Prigent,[4] T. Sachs,[5,6] C. A. R. Corradi,[7] F. J. W. Parmentier,[1] and A. J. Dolman[1]

[1] Methane (CH$_4$) emission from boreal, arctic and subarctic wetlands constitutes a potentially positive feedback to global climate warming. Many process-based models have been developed, but high uncertainties remain in estimating the amount of CH$_4$ released from wetlands at the global scale. This study tries to improve estimates of CH$_4$ emissions by up-scaling a wetland CH$_4$ emission model, PEATLAND-VU, to the global scale with a spatial resolution of 0.5° for the period 2001–2006. This up-scaling was based on the global circum-arctic distribution of wetlands with hydrological conditions being specified by a global hydrological model, PCR-GLOBWB. In addition to the daily hydrological output from PCR-GLOBWB, comprising water table depths and snow thickness, the parameterization included air temperature as obtained from the ECMWF Operational Archive. To establish the uncertainty in the representations of the circum-arctic distribution of wetlands on the CH$_4$ emission, several existing products were used to aggregate the emissions. Using the description of potential peatlands from the FAO Digital Soil Map of the World and the representation of floodplains by PCR-GLOBWB, the average annual flux over the period 2001–2006 was estimated to be 78 Tg yr^{-1}. In comparison, the six-year average CH$_4$ fluxes were 37.7, 89.4, 145.6, and 157.3 Tg yr^{-1} for different estimates of wetland extends based on the studies by Matthews and Fung, Prigent et al., Lehner and Döll, and Kaplan, respectively. This study shows the feasibility to estimate interannual variations in CH$_4$ emissions by coupling hydrological and CH$_4$ emission process models. It highlights the importance of an adequate understanding of hydrology in quantifying the total emissions from northern hemispheric wetlands and shows how knowledge of the sub-grid variability in wetland extent helps to prescribe relevant hydrological conditions to the emission model as well as to identify the uncertainty associated with existing wetland distributions.

[1]Department of Hydrology and Geo-Environmental Sciences, Faculty of Earth and Life Sciences, VU University Amsterdam, Amsterdam, Netherlands.

[2]Now at Climate Change Unit, Institute for Environment and Sustainability, DG Joint Research Centre, European Commission, Ispra, Italy.

[3]Department of Physical Geography, Utrecht University, Utrecht, Netherlands.

[4]Département de Radioastronomie Millimétrique, Observatoire de Paris, Paris, France.

[5]Research Unit Potsdam, Alfred Wegener Institute for Polar and Marine Research, Potsdam, Germany.

[6]Now at Helmholtz Centre Potsdam, German Research Centre for Geosciences, Potsdam, Germany.

[7]Laboratory of Forest Ecology, Department of Forest Environment and Resources, University of Tuscia of Viterbo, Viterbo, Italy.

1. Introduction

[2] Northern latitudes above 50°N contain 53% of the global wetland area [*Aselmann and Crutzen*, 1989]. Wetlands are thought to be the largest natural source of methane (CH$_4$) second only to natural CH$_4$ seeps/geologic emissions [*Etiope et al.*, 2002]. The largest anthropogenic source stems from rice agriculture, ruminants, and energy production [*IPCC*, 2001]. In relatively cold non-aerated waterlogged soils, anaerobic conditions can drastically reduce microbial respiration rates, leading to the accumulation of soil organic matter and CH$_4$ emission. CH$_4$ is a much stronger greenhouse gas than carbon dioxide (CO$_2$) on a molecular basis and has a twenty times larger radiative forcing than CO$_2$ [*IPCC*, 2007]. The total global CH$_4$ source is relatively well constrained from atmospheric observations but the strength

Table 1. Estimates of Global Northern Hemispheric CH₄ Emissions From Natural Wetlands[a]

Literature Source	CH₄ Estimate (Tg yr^{-1})	Extent	Method
Khalil and Rasmussen [1983]	150 ± 50	natural global wetlands	model simulations
Seiler [1984]	13–57	natural global wetlands	measurements
Sebacher et al. [1986]	45–106	natural global wetlands	measurements
Matthews and Fung [1987]	~60% of ~110 = ~66	peat-rich bogs 50–60°N	global wetland database from digital sources
Fung et al. [1991]	35	wetlands and tundra poleward of 50°N	compilation of CH₄ flux measurements
Christensen et al. [1996]	18–30	sub-arctic tundra	CH₄ flux measurements
Bartlett and Harris [1993]	38	northern wetlands north of 45°N	from extensive flux data base and the wetland areas compiled by *Matthews and Fung* [1987]
Cao et al. [1996]	24	northern wetlands	process-based ecosystem model
Walter et al. [2001]	25% of 260 = 65	wetlands above 30°N	process based CH₄ model
IPCC [2001]	115–237	(global wetlands) and 1/3 to 1/2 of it from northern wetlands, north of 50°N	model estimates
IPCC [2007]	~60% of 200 = ~120	northern wetlands	model estimates
Wania et al. [2010]	40 to 74	45–90°N	coupled vegetation model and CH₄ model
PCR-GLOBWB [2009] (based on FAO/ISRIC approach)	78 ± 3.3	wetlands and floodplains above 30°N	coupling between a CH₄ model and a global hydrological model
PCR-GLOBWB [2009] (based on *Lehner and Döll*'s [2004] approach)	145.6 ± 14.9	wetlands and floodplains above 30°N	coupling between a CH₄ model and a global hydrological model
PCR-GLOBWB [2009] (based on *Matthews and Fung*'s [1987] approach)	37.7 ± 2.5	wetlands and floodplains above 30°N	coupling between a CH₄ model and a global hydrological model
PCR-GLOBWB [2009] (based on *Prigent et al.*'s [2007] approach)	89.4 ± 6.6	wetlands and floodplains above 30°N	coupling between a CH₄ model and a global hydrological model
PCR-GLOBWB [2009] (based on *Kaplan*'s [2002] approach)	157.3 ± 7	wetlands and floodplains above 30°N	coupling between a CH₄ model and a global hydrological model

[a]The CH₄ values are in chronological order and aim to show the global picture of literature based budgets. The last estimates are the results of this study, applying the five different approaches as described by this paper.

and trends of the contributing sources are considerably less known [*IPCC*, 2007].

[3] During the last decades several studies attempted to estimate the global budget of CH₄ for wetlands. *Khalil and Rasmussen* [1983] (as cited by *World Meteorological Organization* [1986]) estimated an annual CH₄ emission rate from wetlands of 150 ± 50 Tg yr^{-1}. *Seiler* [1984] estimated that northern wetlands produce annually 11 to 57 Tg CH₄. In all these studies, the total area of northern wetlands varies between 2.6×10^{12} m² [*Twenhofel*, 1926, 1951] and a maximum of 9.0×10^{12} m² [*Sebacher et al.*, 1986]. *Fung et al.* [1991] and *Bartlett and Harris* [1993] estimated an emission rate of 35 Tg yr^{-1} from the northern wetlands. Measurements from boreal and sub-arctic wetland regions reveal an annual emission rate between 0.5 and 10 g CH₄ m^{-2} yr^{-1} [*Crill et al.*, 1988; *Moore and Knowles*, 1987, 1990; *Sebacher et al.*, 1986; *Whalen and Reeburgh*, 1988]. These studies put the estimate of CH₄ emission from wetlands in the range between 11 and 300 Tg yr^{-1} [*Matthews and Fung*, 1987].

[4] More recently models have been developed to estimate CH₄ emission from northern wetlands. The study by *Cao et al.* [1996] was one of the first to apply a process-based CH₄ model that simulated CH₄ emissions based on the amount of decomposed organic carbon, water table, and temperature. *Cao et al.* [1996] estimated a global CH₄ emission

of 145 Tg yr^{-1}, of which 24 Tg yr^{-1} originated from natural wetlands (Table 1).

[5] Using a process-oriented ecosystem source model based on heterotrophic respiration, *Christensen et al.* [1996] estimated a CH₄ flux of 20 Tg yr^{-1} from northern wetlands (>50°N).

[6] To be able to simulate interannual variation in CH₄ emission from natural wetlands, *Walter et al.* [2001] developed a process-based model that derives CH₄ emission from natural wetlands as a function of soil temperature, water table, and net primary production (NPP). In addition, a simple hydrologic model (bucket type) was developed to simulate the position of the water table in wetlands. The model was validated against data from different wetland sites. Using the global wetland distribution map of *Matthews and Fung* [1987], they estimated the global annual CH₄ emission from wetlands to be 260 Tg yr^{-1} of which 25% originated from wetlands north of 30°N.

[7] The seasonal and interannual variation in wetland area remains one of the largest uncertainties in the global CH₄ budget, in particular for the roughly 60% of wetlands that are inundated only for a specific period of the year. Characterizing global inundated wetlands and their dynamics is extremely difficult because wetlands comprise a broad range of environments. Existing global data sets of natural wetlands area and rice cultivation [e.g., *Matthews and Fung*,

1987; *Matthews et al.*, 1991; *Cogley*, 1991] represent wetland distribution based on vegetation and soils but rely on incomparable wetland definitions [*Prigent et al.*, 2001]. *Lehner and Döll* [2004] developed and validated a global database of lakes, reservoirs and wetlands (GLWD) based on different available cartographic sources. *Kaplan* [2002] used the BIOME4-TG model, an equilibrium-state terrestrial biosphere model that couples biogeography and biogeochemistry, to calculate the vegetation distribution in response to both changing climate and atmospheric CO_2 concentrations. To define wetlands, *Kaplan* [2002] used a simple empirical algorithm that selected as wetlands those grid cells that were sufficiently flat (slope < 0.3%) and sufficiently wet on a monthly basis (relative degree of saturation >65%). He then calculated CH_4 emission as a fraction of heterotrophic respiration, R_h [*Christensen et al.*, 1996].

[8] *Gedney et al.* [2004] studied the potential for wetland emissions to feedback on climate change by including an interactive wetlands scheme that was radiatively coupled to an integrated climate model. The scheme predicted wetland area and CH_4 emissions from soil temperature and water table depth, and was optimized to reproduce the observed inter-annual variability in atmospheric CH_4. *Gedney et al.* [2004] created a simple CH_4 emission scheme coupled to the land surface scheme MOSES-LSH which parameterizes the CH_4 flux from wetlands including basic control through temperature, water table and soil carbon. Their results predict a considerable increase in the CH_4 emissions and suggest that these may reach ~500–600 Tg CH_4 yr^{-1} by the year 2100. The total wetland area decreased only slightly by 2100 in their study, suggesting that the response to increased wetland temperature is more important in changing the CH_4 emissions than the increase in wetlands. *Bergamaschi et al.* [2007] developed a new wetland map by assembling the best available source of large-scale wetland cover information for each continent or region. In this way they created a globally consistent data set defining the presence or absence of wetland. To calculate the CH_4 emissions they used the algorithm described by *Christensen et al.* [1996] and *Kaplan* [2002].

[9] Recently, *Wania et al.* [2010] modified the LPJ (Lund-Potsdam-Jena) dynamic global vegetation model to simulate permafrost dynamics, peatland hydrology and peatland vegetation. She used the model to study the dynamics of the active layer depth, water table regimes and vegetation in northern peatlands. A CH_4 model was also developed and coupled with the LPJ hydrology-vegetation model resulting in the LPJ-Why model. The results were tested against five sites and the calculated CH_4 fluxes for 45°N–90°N varied between 40 and 74 Tg CH_4 yr^{-1}.

[10] Adequate specification of hydrological processes is a crucial factor in the production of CH_4 released from northern wetlands [e.g., *Petrescu et al.*, 2008]. However, actual data on water table dynamics are generally not available for large areas and the associated hydrological regimes have to be modeled using climatic data. In the present study, the coupling between a processed based CH_4 model and a global hydrological model aims to calculate the pan-arctic CH_4 emission from floodplains and wetlands, consisting of bogs, fens and mires, for the Northern Hemi-

sphere. We used the dynamic PCR-GLOBWB water table and wetland extent simulations, while the CH_4 budgets were calculated with the process based CH_4 emission model, PEATLAND-VU.

2. Methods

[11] We coupled the macro-scale hydrological model PCR-GLOBWB [*van Beek*, 2007] to the CH_4 emission model PEATLAND-VU [*van Huissteden et al.*, 2006] (Figure 1). The models are applied with a spatial resolution of 0.5° and a daily time step, for the period 2001–2006. The daily CH_4 emission rates were then aggregated to monthly values for each 0.5° cell, thus giving the spatiotemporal distribution of CH_4 emissions for the full northern circumarctic hemispheric domain. In this study, this area encompasses the Northern Hemisphere landmass with a mean annual temperature of less than 5°C.

[12] PEATLAND-VU is a process-based model of CO_2 and CH_4 emission from peat soils under various management scenarios [*van Huissteden et al.*, 2006]. It includes, among others, a modified version of the *Walter and Heimann* [2000] soil profile scale emission model [*van Huissteden et al.*, 2006] and a simplified soil physical model to simulate soil temperatures and soil freezing/thawing. The site-specific soil parameters are hard to obtain for the entire area under consideration. Therefore, we used the same soil parameters as published by *Petrescu et al.* [2008] and slightly decreased the CH_4 production rate R_0. The R_0 is controlled by the amount of substrate present in the soil and it becomes a de facto tuning parameter, which has to be calibrated to obtain the right amplitude of the CH_4 emissions [*Walter and Heimann*, 2000].

[13] Since wetlands vary widely in hydrologic, soil and vegetation characteristics, a distinction was made between bogs, mires and fens on the one hand and floodplains on the other. The first group, bogs and mires, although quite diverse in itself, experiences flooding as a result of local precipitation and groundwater and receives a limited nutrient supply [*Charman*, 2002]. The second group floods as a result of elevated river discharge, importing sediment and nutrients from elsewhere. Thus, floodplains tend to have mineral soils and can sustain more productive vegetation. These differences may induce higher CH_4 fluxes from floodplains [*van Huissteden et al.*, 2005; *van der Molen et al.*, 2007]. Hence, separate parameterizations of soil and vegetation characteristics exist in PEATLAND-VU for wetlands and floodplains respectively (see Text S1).[1]

[14] For each 0.5° cell and wetland type, the hydrological conditions for PEATLAND-VU are prescribed as time series by the PCR-GLOBWB model. This is a macro-scale hydrological model that calculates the water storage on a cell-by-cell basis in two vertically stacked soil layers and an underlying groundwater reservoir. The exchange between the soil column and the atmosphere includes rainfall, snowmelt and evaporation from plants and interception while drainage from the soil column is routed along a

---

[1] Auxiliary materials are available with the HTML. doi:10.1029/2009GB003610.
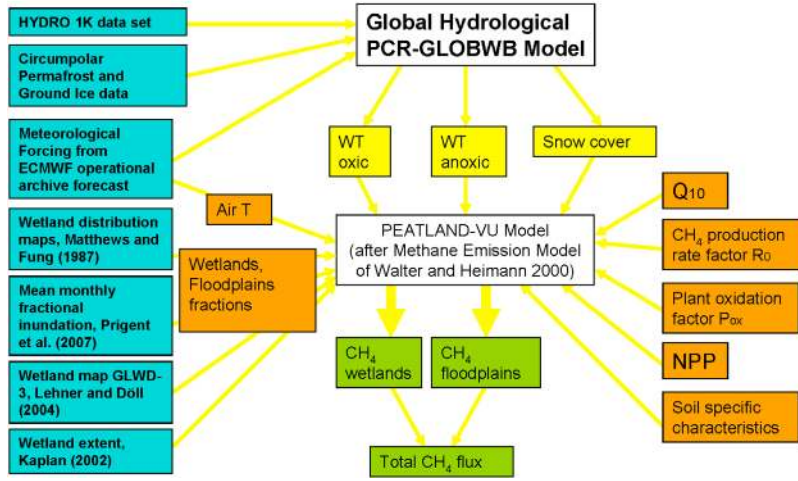
Processes PCR-GLOBWB + PEATLAND-VU

Figure 1. Diagram describing the coupling of PEATLAND-VU and PCR-GLOBWB. Shown are spatial input (maps, cyan), location specific parameterization for PEATLAND-VU (time series and tables, orange) and output (time series, green). Arrows (yellow) indicate the direction of information exchange. Output time series have subsequently been processed and aggregated to obtain maps of CH₄ fluxes for different periods. We define wetlands as bogs, fens and mires.

drainage network [*van Beek*, 2007]. The meteorological forcing of PCR-GLOBWB consists of daily forecast fields of precipitation, air temperature and actual evapotranspiration from the ECMWF Operational Archive for the period 2000–2006. Two hydrological situations were considered: a fully saturated or anoxic profile and an unsaturated oxic one. Anoxic conditions are specified by the mean height of the floodwaters, oxic conditions by the depth of the water table relative to the soil surface. The height of the floodwaters over the floodplain and the extent of flooding were calculated using the HYDRO 1k data set [*Verdin*, 1997] (HYDRO 1K Elevation Derivative Database and GCIP/EOP Land Characterization is available at http://data.eol.ucar.edu/codiac/dss/id=21.078; HYDRO 1K data set is available at http://eros.usgs.gov/#/Find_Data/Products_and_Data_Available/gtopo30/hydro). For sub-catchments smaller than the 0.5° cells, the relative height above the floodplain of each 1 km cell was calculated. For each cell, the aggregated sub-grid distribution was then represented by percentiles (0.01, 0.05 and 0.1 through 1.0 by increments of 0.1). This distribution was applied a posteriori to the river stages that were simulated by PCR-GLOBWB for a fixed floodplain extent based on a blended data set of the GLWD1 and the HYDRO 1k data set [*Lehner and Döll*, 2004; *Verdin*, 1997]. The height of the floodwaters and the extent of the submerged area then follow from intersecting the cumulative floodplain volume with the discharge in excess of channel storage.

[15] For the wetlands, the extent of the inundated area characterized by anoxic conditions was calculated by the improved Arno Scheme of *Hagemann and Gates* [2003]. This scheme calculates the saturated fraction as the area under the cumulative soil depth distribution that becomes saturated when the local storage capacity is exceeded by the cell-averaged moisture storage (Figure 2). As the moisture storage changes, so will the storage capacity and the saturated fraction. Thus, the oxic and anoxic parts are given by equations (1) and (2):

$$x_{sat} = \min(x_t, x_{t+1}) \tag{1}$$

$$x_{unsat} = |x_t - x_{t+1}| \tag{2}$$

where x_{sat} is the saturated, *anoxic*, part of the cell and x_{unsat} is the unsaturated, *oxic*, part; t, and t + 1 represent the previous and present time step respectively.

[16] The height of the floodwaters was estimated by the average water storage in excess of the water holding capacity of the soil. The corresponding water height, *h*, is given by:

$$h_{sat} = \frac{1}{2}(w_{t+1} - w_{\min}) \tag{3}$$

which represents the ponded water level on top of the anoxic part, taken as the average between *w* at t + 1 and the minimum water storage capacity;

[17] In case of flooding, $(x_{t+1} > x_t)$, the previously oxic profile floods as the ponded water level rises:

$$h_{unsat} = \frac{1}{2}(w_{t+1} - w_t) \tag{4}$$

In case of drainage, $(x_{t+1} < x_t)$, the anoxic profile changes partly to oxic with the corresponding water depth given by:

$$h_{unsat} = \frac{1}{2}(w_{t+1} - w_t)\frac{\sum_i z_i}{\sum_i z_i(\theta_{sat} - \theta_{FC})} \tag{5}$$
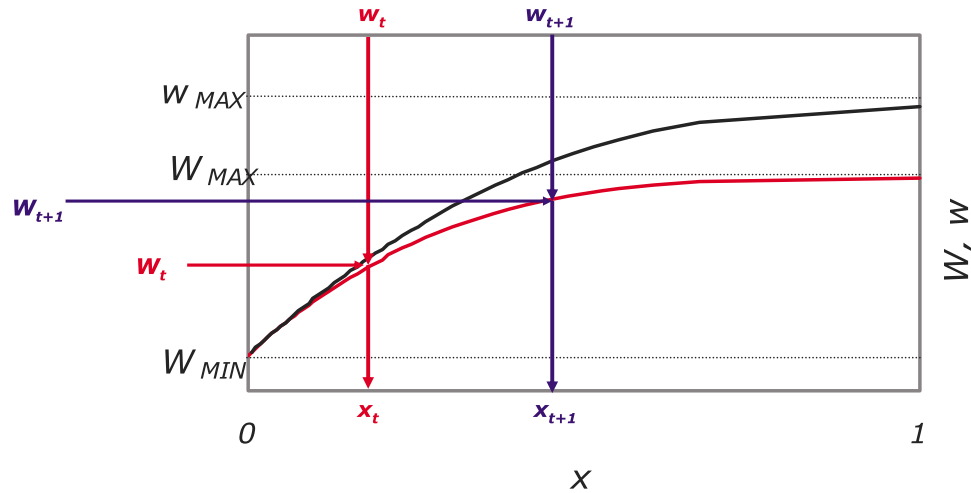
Figure 2. The functioning of the improved Arno Scheme: w represents the distribution of the local water holding capacity, and W represents the area-averaged value. The minimum and maximum storage capacities are also indicated. As long as the actual water storage (w_t, W_t) is less than w_{min}, the fractional saturation, x_t, is zero. If equal to the maximum available value, the entire area becomes saturated ($x_t = 1$). Arrows indicate how, with increasing water storage, the saturated area increases. This principle and the excess water storage over the saturated fraction are used to simulate the oxic and anoxic fractions in the coupling between PCR-GLOBWB and PEATLAND-VU.

which is the water depth when the water level falls below the soil surface. This is obtained by dividing it with the difference between saturation and field capacity ($\theta_{sat} - \theta_{FC}$), subsequently weighted by the respective depths of the layers

$$\rho_{Snow} = \frac{\frac{1}{2}\left(\rho_{Snow}(t) + \rho_{Snow}(t-1)\right) \times Z_{SnowWE}(t-1) + \rho_{Snow}(t = 0) \times \Delta Z_{SnowWE}(t) + \rho_w \times Z_{SnowLiqWE}(t)}{Z_{SnowWE}(t-1) + \Delta Z_{SnowWE} + Z_{SnowLiqWe}} \tag{7}$$

(z_i); w is the water storage capacity at past, t, and present time step, $t + 1$, respectively and θ is the volumetric moisture content (m³ m⁻³) for each soil layer.

[18] For both wetlands and floodplains, the area represented by oxic conditions is defined as the area that floods or drains depending on whether the inundated area is expanding or contracting. Since the depth of the water table depends on local conditions only, the Arno Scheme was used for both floodplains and wetland. To parameterize the soil physical model of PEATLAND-VU, snow depth data from PCR-GLOBWB are used in combination with the 2 m air temperature of the ECMWF Operational Archive. More details can be found in Text S2.

[19] Water equivalent snow cover was divided by the density of snow to obtain the depth of the snowpack:

$$Z_{Snow} = \frac{Z_{SnowWE}}{\rho_{Snow}} \tag{6}$$

where Z_{Snow} is the depth of the snowpack in m per m², $Z_{Snow\ WE}$ is the water equivalent snow cover and ρ_{Snow} is the density of snow in kgm⁻³.

[20] Snow density is dependent on the age of the snow, changing from 100 kgm⁻³ for fresh snow to 350 kgm⁻³ after 120 days. The development of snow density with age was prescribed as:

where $\rho_{Snow}(t-1)$, $\rho_{Snow}(t)$ and $\rho_{Snow}(t = 0)$ are the densities of the maturing snow for the previous and present-day and for freshly fallen snow, respectively and ρ_w is the density of any liquid water retained by the snowpack. These densities are weighed on the basis of water equivalent depths, being the snow cover handed down from the previous time step, $Z_{Snow\ WE}$ (t−1), any freshly fallen snow for the current time step, $\Delta Z_{Snow\ WE}$ (t), and the retained liquid water in the snowpack, $Z_{SnowLiq\ WE}$ (t). Thus, maturation and melt result in a denser snowpack while any fresh snow will lower its density.

[21] To remove errors from the initial conditions (mainly caused by errors in the temperature profiles), the year 2000 was used to spin up PEATLAND-VU. This effectively limits the analysis to the period 2001–2006. Coupled with PCR-GLOBWB, PEATLAND-VU calculates four time series of CH₄ fluxes per 0.5° cell, for floodplains and wetlands under respectively oxic and anoxic conditions (for site characteristics, see Tables S1 and S2). To obtain the average flux per 0.5° cell, the fluxes per unit area of a particular surface condition were weighed by the fractions of potential

wetland type and hydrological conditions and then aggregated over longer periods:

$$\overline{J}_{CH_4} = \frac{1}{N} \sum_d^N \sum_w f_w \sum_S x_{w_d}^S J_{w_d}^S \qquad (8)$$

where $\overline{J}_{CH_4}$ is the average CH$_4$ flux in g·m^{-2}·d^{-1}, f is the fractional cover per wetland type, x the fractional cover of the wetland area experiencing oxic or anoxic conditions (f and x both in m^2·m^{-2}), and J is the flux per day. The subscript w denotes the wetland type, d the daily time step adding up to N days per month or year, and the superscript s the oxic and anoxic conditions per wetland type. To obtain the final CH$_4$ estimates, the fluxes were multiplied by the cell area.

[22] Inclusion of the potential wetland type was necessary as the parameterization of the improved Arno Scheme in PCR-GLOBWB includes other areas with shallow soils (e.g., urbanized areas or rocky soils). To identify potential wetland areas in PCR-GLOBWB, we used the modified FAO Digital Soil Map of the World- ISRIC [*Batjes*, 1997, 2002] and identified the soil units *gleysols*, *histosols* and those with a *gleyic* phase as areas with poor drainage [cf. *Matthews and Fung*, 1987] and converted their frequency to fractional extent. Since PCR-GLOBWB considers the distribution of the floodplain elevations in detail, potential floodplains were not constrained beforehand. Only when the sum of the fractional floodplain cover and the wetlands exceeded unity, the floodplain area was assumed to encroach onto the wetland area and the corresponding area treated as floodplain.

[23] To establish the robustness of the parameterizations of PCR-GLOBWB, we compared the resulting wetland areas with well known static descriptions of wetland extent, including those of *Matthews and Fung* [1987], *Lehner and Döll* [2004] and *Kaplan* [2002]. In the case of *Kaplan*'s [2002] approach, we replaced his implicit assumption on saturation by the explicit fraction of saturation excluding other impervious surfaces (e.g., urban areas) as included by PCR-GLOBWB. We also compared it with a remote sensing based dynamic approach based on the work of *Prigent et al.* [2007]. Detailed description of all data sets can be found in Text S3 and the wetland extent maps in Figures S1–S5, respectively). We also compared our simulations with observed CH$_4$ fluxes from four arctic sites. Results are shown in mg m^{-2} d^{-1}, the original unit of measurement, in Figure S13–S16 and Table S4. Dependent on the site description and characteristics (Text S5 and Table S5) and their soil physical properties, we used the flux over the anoxic profile of the floodplain or wetland parameterization (Tables S1 and S2).

3. Results

3.1. Potential Wetland Extent and CH$_4$ Distribution Maps

[24] The selected domain of the Northern Hemisphere landmass limited by the 5°C boundary comprises 23564

0.5° cells and covers 32×10^{12} m^2 (Figure S2, gray area). For each of the different wetland data sets this area was further restricted to the extent of the wetlands and floodplains. Using the wetland distribution based on the FAO (ISRIC) map, the data set closest to the parameterization of PCR-GLOBWB, the average boreal wetland area contributing to CH$_4$ emissions was estimated to be 2.97×10^{12} m^2. Using the wetland extent of *Lehner and Döll* [2004] this became 3.42×10^{12} m^2 and 2.44×10^{12} m^2 for *Matthews and Fung* [1987]. Using the mean monthly inundated area of *Prigent et al.* [2007], the calculated mean area was 4.37×10^{12} m^2 while the estimate based on *Kaplan*'s [2002] algorithm was 2.16×10^{12} m^2.

[25] Figure 3 shows the averaged CH$_4$ flux for all approaches over the years 2001–2006, in g m^{-2} d^{-1}. Based on the underlying data, we calculated the annual CH$_4$ budgets, in Tg yr^{-1} as shown in Figure 4 and Table S3. We can observe a similar trend for the five approaches with the years 2001 and 2006 having the highest emission while 2004 has the lowest flux in three of the five approaches.

[26] In Figures S6–S11, we present detailed maps showing the spatial-temporal variations in the annual CH$_4$ fluxes and monthly maximum CH$_4$ fluxes for all approaches.

[27] To identify wetland areas that contribute the most to the overall CH$_4$ emission, we plotted the cumulative sums of CH$_4$ emissions calculated with our coupled models, PCR-GLOBWB/FAO (ISRIC) and PEATLAND-VU. This calculation was done for the year 2006 and averaged over longitude bands. The wetland areas which contribute the most to the global CH$_4$ emissions are found between 60°N and 80°N. (Text S4 and Figure S12).

3.2. Evaluation of the Results

[28] We evaluated the simulations performed with the PCR-GLOBWB/FAO (ISRIC) parameterization against the results presented by *Roulet et al.* [1994]. They executed a measurement campaign in the Hudson Bay Lowlands (HBL) over an area of 320.000 km^2 (the second biggest wetland in the Northern Hemisphere, after the Western Siberian Lowlands, 540.000 km^2). The measurements were done by aircraft during the snow free months of 1990, using airborne eddy correlation techniques [*Roulet et al.*, 1994]. The total HBL annual emissions were estimated to be 0.538 ± 0.187 Tg CH$_4$ yr^{-1}.

[29] We extracted our results from the corresponding area (77°–94°W, 50°–58°N) covering 405330 km^2 (Figure 5). Our estimate of the average annual emission is 2.03 ± 0.18 Tg CH$_4$ yr^{-1}, ranging from 1.7 Tg CH$_4$ yr^{-1} in 2004 and 2.2 Tg CH$_4$ yr^{-1} in 2005 and 2001. This is higher than *Roulet et al.* [1994] estimates from 1990. *Worthy et al.* [2000] concluded, after calculating the CH$_4$ fluxes for the same HBL as ~0.25–0.5 Tg yr^{-1}, that the measured fluxes were much lower than fluxes derived empirically by different models and were more sensitive to temperature. Our model appears to overestimate the fluxes for this area around four times. However, given the uncertainty in the data and the time difference between the data and the modeled years, we can only realistically compare orders of magnitude.
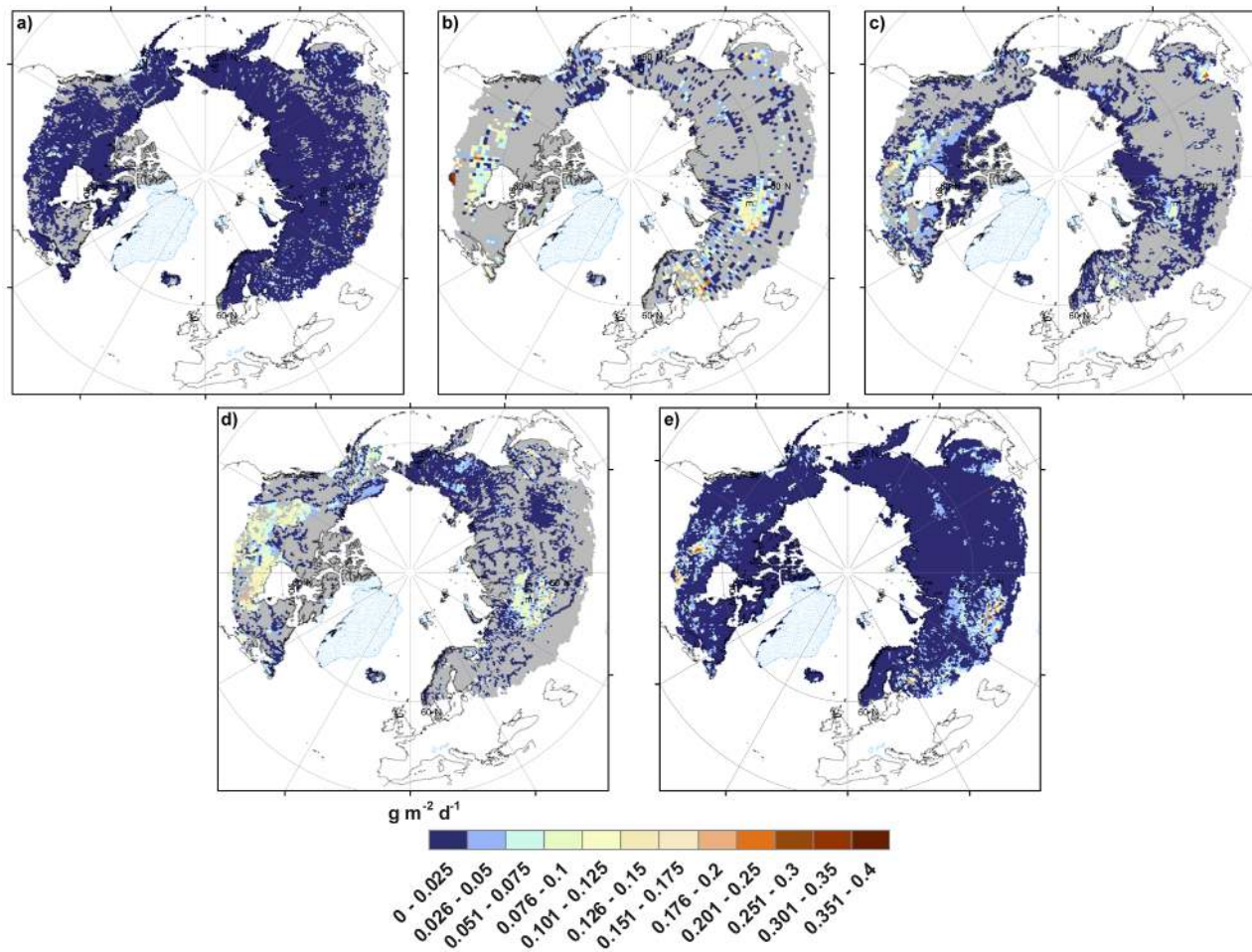
Figure 3. CH₄ distribution maps calculated with (a) PCR-GLOBWB using as input the FAO/ISRIC soil map; (b) *Matthews and Fung* [1987]; (c) *Prigent et al.* [2007]; (d) *Lehner and Döll* [2004]; and (e) *Kaplan* [2002] parameterizations. Each map represents the distribution of the six years average CH₄ flux in g CH₄ m⁻² d⁻¹. The gray area represents maximum extent of global boreal wetland area as defined by the 5°C limit.

[30] Observed flux data from a model intercomparison study are shown in Table S4. For the PCR-GLOBWB estimates of the arctic sites Cherskii, Kytalyk and Stordalen, the model performs well, even if there is still some disagreement with the observed data. This can be caused for instance by individual rain showers or peaks caused by the ebullition that are not captured by the model. For the Lena Delta site the simulations overestimate the measurements (Figure S13). The comparison with the other approaches shows that the results differ widely, none of them in itself comparing well to the measurements.

4. General Discussion

[31] This study aimed at quantifying CH₄ emissions from the Northern Hemisphere by coupling a global hydrological model, PCR-GLOBWB, with a wetland CH₄ emission model, PEATLAND-VU. By calculating fluxes for different existing data sets of circum-arctic wetland extent [*Matthews*

and Fung, 1987; *Lehner and Döll*, 2004; *Prigent et al.*, 2007; *Kaplan*, 2002] as well as for the extent underlying the parameterization of PCR-GLOBWB (FAO), we have been able to identify the uncertainty in variations of CH₄ emissions under given hydrological conditions.

[32] Our main approach was based on simulating the CH₄ emissions using the water table and snow cover output from PCR-GLOBWB as input into the PEATLAND-VU model. Because the PEATLAND-VU model was developed from the plot-scale model of *Walter and Heimann* [2000], it remains a major challenge to define the optimum parameters for PEATLAND-VU model and run the model for the area of interest. The precise effect of introducing a spatially uniform parameter set, instead of one calibrated on particular sites is unknown. *van Huissteden et al.* [2009] tested the PEATLAND-VU model using the GLUE methodology (Generalized Likelihood Uncertainty Estimation) [*Lamb et al.*, 1998; *Beven*, 2001] and references therein) with validation data from different sites, including temperate and
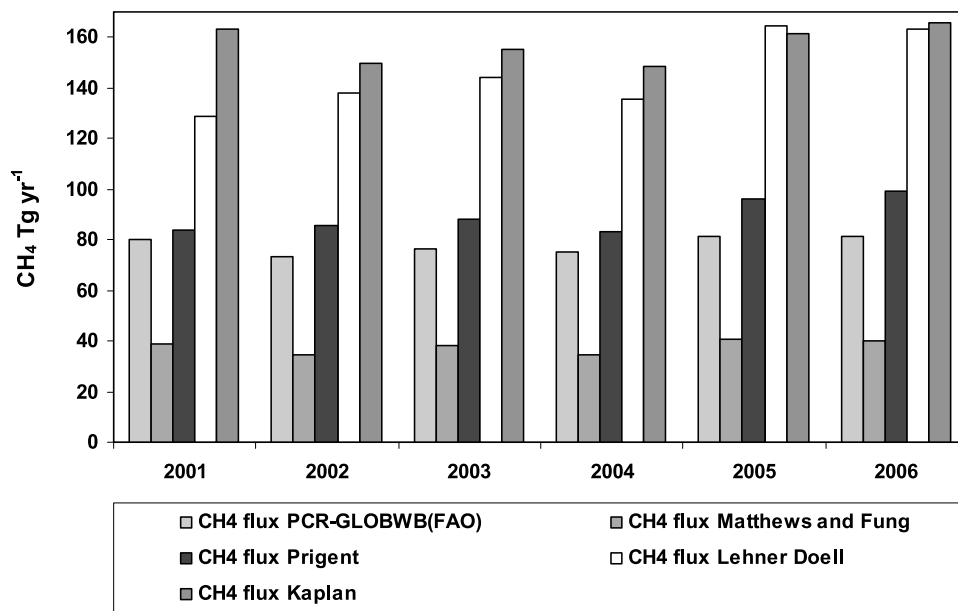
Figure 4. Annual CH$_4$ fluxes (Tg yr^{-1}) calculated with PCR-GLOBWB for the FAO/ISRIC based wetlands, *Matthews and Fung* [1987], *Lehner and Döll* [2004], *Prigent et al.* [2007] and *Kaplan* [2002] parameterizations.

permafrost wetlands. The PEATLAND-VU model was evaluated against a data set using a large number of runs with randomly selected parameters [*van Huissteden et al.*, 2009]. The results showed that the model has more predictive power than a simple emission factor approach. However, there was considerable interaction between parameters

and equifinality of model solutions, implying that different parameter sets may yield similar results.

[33] Since the model runs were usually localized well within the error margin of the data, this suggests that with a well-chosen uniform parameter set the model is able to estimate the emission rate adequately. For our case, errors may be expected to be somewhat larger for the floodplains
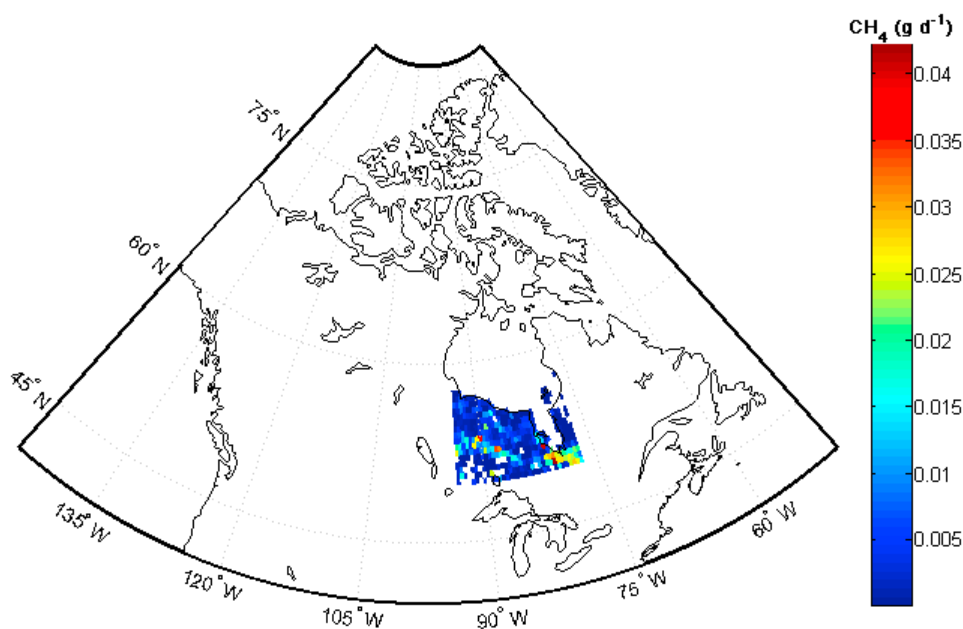

Figure 5. Six year averaged CH$_4$ flux (g d^{-1}), Hudson Bay lowlands, calculated with PCR-GLOBWB (FAO/ISRIC) approach.

than for the other wetlands, because the GLUE analysis suggested a higher uncertainty for eutrophic, high-flux sites (Figure S14).

[34] CH$_4$ fluxes are notoriously variable, both spatially and temporally. Although observed magnitudes of fluxes are generally related to water table, soil temperature and vegetation, the variability of fluxes between measurement points with similar soil type, vegetation and water table position is still extremely high [e.g., *van Huissteden et al.*, 2005; D. M. D. Hendriks et al., Vegetation as indicator for methane emissions, carbon dioxide fluxes and greenhouse balances from peat land, submitted to *Ecohydrology*, 2009]. Sub-daily temporal variations in CH$_4$ fluxes exist and currently cannot be modeled; they are probably related to small-scale differences in vegetation and soil characteristics. Therefore it can be argued that the model should reproduce the average flux of a group of similar points, rather than measurements at a single location. In particular short-lived ebullition events are difficult to reproduce exactly at the right magnitude and time [*Walter et al.*, 2007].

[35] When we compare our yearly trends of CH$_4$ emissions for all approaches (Figure 4) we see that the spatial variation is not very pronounced between the years as the main CH$_4$ contribution comes from same area each year. Most of the variation can be observed in the maps showing the maximum monthly flux (Figure S11). For instance, the PCR-GLOBWB- PEATLAND-VU simulated fluxes tend to be higher in the southern part of the boreal zone, as a result of higher soil temperatures (Figure S12). The PCR-GLOBWB approach uses more spatial detail (HYDRO 1K for floodplain flooding) and recent (2001–2006) climate data. The distribution of the CH$_4$ fluxes using *Kaplan*'s [2002] approach (Figure S10) is similar to the PCR-GLOBWB taking more into account the soil temperature effects. The wetland extent map based on remote sensing data [*Prigent et al.*, 2007] differs from the cartography-based inventories of *Matthews and Fung* [1987] and *Lehner and Döll* [2004] as shown in Table S3. The results based on the *Matthews and Fung* [1987] wetland distribution show that the Western Siberian lowlands and the Baltic Shields with their widespread ombrotrophic wetlands stand out as a major CH$_4$ emission area. For the *Lehner and Döll* [2004] data set the main emissions come from the Western Siberian lowlands and the Canadian lowlands. The same CH$_4$ distribution pattern holds to a smaller extent for the *Prigent et al.* [2007] data set. Some of the high emissions of southern wetlands are obtained by some approaches but not by all since not all of them classify those areas as wetlands. We expect that this is caused by a different vegetation type dominating those areas which is not included in the models.

[36] We compared our results with the other available sets used to validate the CH$_4$ emissions. Using the data set of *Matthews and Fung* [1987], which consists of three different cartographic sources to yield the wetland extent, our results (37.7 Tg CH$_4$ yr^{-1}, averaged over 2001–2006) are half of the estimates made 20 years ago (60% of the total of 110 Tg CH$_4$ yr^{-1} = 66 Tg yr^{-1} originate from peat rich bogs concentrated from 50 to 70°N). They are primarily lower due to the difference in calculated area. The area used by *Matthews and Fung* [1987] was 3.7×10^{12} m^2 while PCR-GLOBWB's estimated area for this approach was 2.44×10^{12} m^2. According to *Matthews and Fung* [1987] the area of wet tundra between 70 and 80°N is about 0.1×10^{12} m^2. This area was estimated by *Fung et al.* [1991] to contribute with 3% of the total of 30 CH$_4$ Tg yr^{-1} which is 1 Tg yr^{-1}. If we apply this hypothesis to PCR-GLOBWB calculation we get an estimate of 2.4 Tg yr^{-1} over the same area. The difference between the two estimates may be caused by the different estimation methods or alternatively imply that compared to the 1990s, the CH$_4$ emissions have increased. This may be caused by changes in hydrological conditions and temperature as incorporated in our models. The same increase was noticed from the comparison performed on the Hudson Bay Lowlands where we obtained a CH$_4$ emission rate twice as high compared to the one from 1990. This is in line with *Bousquet et al.* [2006] who concluded that atmospheric CH$_4$ levels may increase in the near future if wetland emissions return to their mean 1990s levels.

[37] *Prigent et al.* [2007] use information from multiple satellites to derive monthly averages of fractional inundation over the years 1993–2000. We processed our emissions with this data set and calculated the emissions for 2001–2006. This data set gives information on the maximum inundation extent but not on how long inundation persists during the month, which may particularly bias our analysis as we use monthly values that are averages over the entire observation period. This might be one of the reasons why our calculation of the CH$_4$ budget (89.4 Tg CH$_4$ yr^{-1} averaged over 2001–2006) is one of the highest estimates. There is still some uncertainty in estimating the inundation extent for a single cell as the timing and the duration of the flooding conditions are still unclear. This uncertainty also pertains to the other approaches. More observations are needed of the vegetation changes and estimation of the inundated area [*Prigent et al.*, 2001]. The inundated area reported by *Prigent et al.* [2007] was 1.6×10^{12} m^2 for 55°–70 °N. We calculated a possible mean wetland area for the northern hemisphere of 4.37×10^{12} m^2 for $T_{avg} < 5$°C. Unlike *Matthews and Fung* [1987] where inundated area comes from cartographical charts and which probably accounts for the warm season of maximum flooding, the *Prigent et al.* [2007] data set does not distinguish among standing water in natural wetlands, rice paddies or rivers and lakes.

[38] *Lehner and Döll* [2004] used the wetland information from a large variety of existing maps (eighteen), generalizing the global information at three different resolutions (GLWD 1–3). For the present study we used the wetland information from the map with the finest spatial detail (GLWD-3 at 30 arc seconds) which contains twelve different classes (see data set description in Text S3).As in the PCR-GLOBWB method based on the FAO-derived wetland extent, the main areas emitting CH$_4$ are toward the south of the Western Siberian lowlands and the south of the HBL. The averaged CH$_4$ emission over the six years was 145.6 Tg yr^{-1}, the second highest estimate of all results. This is mainly caused by the large area of floodplains, defined in the database as classes 4 and 5, which, compared to the other data sets, covers a very large area in North Canada and Western Russia (Figure S4).

[39] Using *Kaplan*'s [2002] empirical approach, PCR-GLOBWB calculated the maximum wetland extent where Kaplan's implicit assumption on saturation would be replaced by the explicit fraction of saturation (excluding other impervious surfaces, i.e., urban areas). With these assumptions, our results become quite high compared to the other calculations, but are close to *Lehner and Döll*'s [2004] approach. Kaplan's model is known to fail to predict the Alaskan wetlands and discontinuous Scandinavian wetlands [*Kaplan*, 2002]. For the CH$_4$ emissions, he calculated a total global budget of 140 Tg yr^{-1}, while our total estimate averaged over the six years was 157.3 Tg yr^{-1} for the area >30°.

[40] In Figure 3e we can observe that, using Kaplan's approach, almost every cell generates a very small CH$_4$ flux since all cells having flat slopes and some saturation will produce a flux that is larger than zero. This is partly due to unresolved detail in other data sets or processes not captured by Kaplan's approach that prevent the formation of wetlands. Importantly, the differences also show that a correct determination of wetland extent is crucial for determining wetland CH$_4$ fluxes.

[41] Because of the sensitivity of the model results to the vegetation parameters [*van Huissteden et al.*, 2009], it would be very interesting to couple our models to a vegetation model [*Wania et al.*, 2010], In comparison to *Wania et al.*'s [2010] estimates we observe that all our estimates are higher than those obtained by a CH$_4$ model coupled to a vegetation model. For 45°–90°N, *Wania et al.* [2010] reports a CH$_4$ emission rate of 40 to 74 Tg yr^{-1} for 1961–1990 for an area 2.99×10^{12} to 3.21×10^{12} m^2.

[42] Our modeling study did not include emissions related to permafrost thaw [*Walter et al.*, 2006; *Zimov et al.*, 2006]. The modeling of permafrost thaw effects would require modeling of geomorphic effects of permafrost thaw such as thaw lake formation [*Khvorostyanov et al.*, 2008; *Walter et al.*, 2006]. However, with our approach, year-to-year variability of wetland CH$_4$ emissions related to changes in precipitation and temperature can be quantified and mapped. For instance, the high CH$_4$ emission of floodplains is highly sensitive to precipitation and discharge variations [*van Huissteden et al.*, 2005] effect which is fully included in our model.

5. Conclusions

[43] The CH$_4$ flux for the northern hemisphere was calculated using five different data sets for wetland extent. Our results varied between a minimum average estimate of 37.7 Tg CH$_4$ yr^{-1} [*Matthews and Fung*, 1987] and a maximum of 157.3 Tg CH$_4$ yr^{-1} [*Kaplan*, 2002] and showed considerable year-to-year variation. Very high emission rates were found above the 65°N line in the Siberian Wetlands, Northern Europe and Canadian lowlands. Compared to existing estimates from Canada, our model overestimated the emissions by a factor of four. Comparing the PCR-GLOBWB simulated results with flux measurements from four sites showed similar averaged values for two out of four sites: Cherskii and Stordalen (see Table S4).

[44] However, errors in quantifying CH$_4$ emission rates when taking into account the different data sets and calculations can be substantial. These are mainly due to 1) the high variability in reported wetland extent; 2) uncertainty in using one global parameter set to model the CH$_4$ emissions (as shown by *van Huissteden et al.* [2009]) and 3) emission processes that are not included in the model (ebullition events). A good estimation of the extent of wetland area together with temperature records is important for calculating realistic CH$_4$ emissions from high latitude wetlands.

[45] Our attempt in calculating the CH$_4$ budgets from the most important natural CH$_4$ source is a step forward in improving calculations of global estimates and wetlands extents. The results from the coupling between a process based CH$_4$ model and a global hydrological model and the results obtained suggest that it is possible, to give a plausible bottom-up estimate of the CH$_4$ budget and its spatial and temporal variation, based on relatively simple approaches, The calculations based on the Lehner and Döll and Kaplan parameterizations are on the high end of published values but estimates based on PCR-GLOBWB/FAO coupled with PEATLAND-VU produced a more plausible estimate.

[46] Further improvements of the model, including a spatially variable parameterization of wetland vegetation characteristics, should be considered. Vegetation characteristics related to plant transport and oxidation of CH$_4$ vary widely on smaller and larger scales. In particular differences between vascular (e.g., sedge and reed-type vegetation) and nonvascular (e.g., peat mosses) may be important [*Raghoebarsing et al.*, 2005; *van Huissteden et al.*, 2005].

References

Aselmann, I., and P. J. Crutzen (1989), Global distribution of natural fresh-water wetlands and rice paddies, their net primary productivity, seasonality and possible CH$_4$ emissions, *J. Atmos. Chem.*, *8*, 307–358, doi:10.1007/BF00052709.

Bartlett, K. B., and R. Harris (1993), Review and assessment of methane emissions from wetlands, *Chemosphere*, *26*, 261–320, doi:10.1016/0045-6535(93)90427-7.

Batjes, N. H. (1997), A world dataset of derived soil properties by FAO-UNESCO soil unit for global modeling, *Soil Use Manage.*, *13*, 9–16, doi:10.1111/j.1475-2743.1997.tb00550.x.

Batjes, N. H. (2002), Revised soil parameter estimates for the soil types of the world, *Soil Use Manage.*, *18*, 232–235.

Bergamaschi, P., et al. (2007), Satellite chartography of atmospheric methane from SCIAMACHY on board ENVISAT: 2. Evaluation based on inverse model simulations, *J. Geophys. Res.*, *112*, D02304, doi:10.1029/2006JD007268.

Beven, K. J. (2001), *Rainfall-Runoff Modelling. The Primer*, 360 pp., Wiley, Chichester, U. K.

Bousquet, P., et al. (2006), Contribution of anthropogenic and natural sources to atmospheric methane variability, *Nature*, *443*, doi:10.1038/nature05132.

Cao, M., S. Marshall, and K. Gregson (1996), Global carbon exchange and methane emissions from natural wetlands: Application of a process-

based model, *J. Geophys. Res.*, 101(D9), 14,399–14,414, doi:10.1029/96JD00219.

Charman, D. (2002), *Peatlands and Environmental Change*, 301 pp., Wiley, Chichester, U. K.

Christensen, T. R., I. C. Prentice, J. Kaplan, A. Haxeltine, and S. Sitch (1996), Methane flux from northern wetlands and tundra: An ecosystem source modelling approach, *Tellus, Ser. B*, 48, 652–661, doi:10.1034/j.1600-0889.1996.t01-4-00004.x.

Cogley, J. C. (1991), GGHYDRO-Global Hydrographic data release 2.0, *Climate Note 91-1*, 12 pp., Trent Univ., Petersborough, Ont., Canada.

Crill, P. M., K. B. Bartlett, R. C. Hariss, E. Gorham, E. S. Verry, D. I. Sebacher, L. Madzar, and W. Sanner (1988), CH₄ flux from Minnesota peatlands, *Global Biogeochem. Cycles*, 2, 371–384, doi:10.1029/GB002i004p00371.

Etiope, G., A. Caracausi, R. Favara, F. Italiano, and C. Baciu (2002), Methane emission from the mud volcanoes of Sicily (Italy), *Geophys. Res. Lett.*, 29(8), 1215, doi:10.1029/2001GL014340.

Fung, I., J. John, J. Lerner, E. Matthews, M. Prather, L. P. Steele, and P. J. Fraser (1991), Three-dimensional model synthesis of the global methane cycle, *J. Geophys. Res.*, 96(D7), 13,033–13,065, doi:10.1029/91JD01247.

Gedney, N., P. M. Cox, and C. Huntingford (2004), Climate feedback from wetland methane emissions, *Geophys. Res. Lett.*, 31, L20503, doi:10.1029/2004GL020919.

Hagemann, S., and L. D. Gates (2003), Improving a subgrid runoff parameterization scheme for climate models by the use of high resolution data derived from satellite observations, *Clim. Dyn.*, 21, 349–359, doi:10.1007/s00382-003-0349-x.

IPCC (2001), *Third Assessment Report. Synthesis Report*, stand-alone edition, edited by R. T. Watson and the Core Writing Team, 184 pp., IPCC, Geneva.

IPCC (2007), *Climate Change. The Physical Science Basis. Contribution of Working Group I to the Fourth Assessment Report of the Intergovernmental Panel on Climate Change*, edited by S. Solomon et al., Cambridge Univ. Press, Cambridge, U. K. (Available at http://www.ipcc.ch/pdf/assessment-report/ar4/wg1/ar4-wg1-chapter2.pdf, last access April 2009)

Kaplan, J. O. (2002), Wetlands at the Last Glacial Maximum: Distribution and methane emissions, *Geophys. Res. Lett.*, 29(6), 1079, doi:10.1029/2001GL013366.

Khalil, M. A. K., and R. A. Rasmussen (1983), Sources, sinks, and seasonal cycles of atmospheric methane, *J. Geophys. Res.*, 88(C9), 5131–5144, doi:10.1029/JC088iC09p05131.

Khvorostyanov, D. V., G. Krinner, P. Ciais, M. Heimann, and S.A. Zimov (2008), Vulnerability of permafrost carbon to global warming. Part I: Model description and role of heat generated by organic matter decomposition, *Tellus, Ser. B*, 60, 250–264, doi:10.1111/j.1600-0889.2007.00333.x.

Lamb, R., K. J. Beven, and S. Myrabø (1998), Use of spatially distributed water table observations to constrain uncertainty in a rainfall-runoff model, *Adv. Water Resour.*, 22(4), 305–317, doi:10.1016/S0309-1708(98)00020-7.

Lehner, B., and P. Döll (2004), Development and validation of a global database of lakes, reservoirs and wetlands, *J. Hydrol.*, 296, 1–22, doi:10.1016/j.jhydrol.2004.03.028.

Matthews, E., and I. Fung (1987), Methane emissions from natural wetlands: Global distribution, area, and environmental characteristics of sources, *Global Biogeochem. Cycles*, 1, 61–86, doi:10.1029/GB001i001p00061.

Matthews, E., I. Fung, and J. Lerner (1991), Methane emissions from rice cultivation: Geographic and seasonal distribution of cultivated areas and emissions, *Global Biogeochem. Cycles*, 5, 3–24, doi:10.1029/90GB02311.

Moore, T. R., and R. Knowles (1987), Methane and carbon dioxide evolution from subarctic fens, *Can. J. Soil Sci.*, 67, 77–81, doi:10.4141/cjss87-007.

Moore, T. R., and R. Knowles (1990), CH₄ emissions from fen, bog and swamp peatlands in Quebec, *Biogeochemistry*, 11, 45–61, doi:10.1007/BF00000851.

Petrescu, A. M. R., J. van Huissteden, M. Jackowicz-Korczynski, A. Yurova, T. R. Christensen, P. M. Crill, K. Bäckstrand, and T. C. Maximov (2008), Modelling CH₄ emissions from arctic wetlands: Effects of hydrological parameterization, *Biogeosciences*, 5, 111–121, doi:10.5194/bg-5-111-2008.

Prigent, C., E. Matthews, F. Aires, and W. B. Rossow (2001), Remote sensing of global wetland dynamics with multiple satellite datasets, *Geophys. Res. Lett.*, 28(24), 4631–4634, doi:10.1029/2001GL013263.

Prigent, C., F. Papa, F. Aires, W. B. Rossow, and E. Matthews (2007), Global inundation dynamics inferred from multiple satellite observations, 1993–2000, *J. Geophys. Res.*, 112, D12107, doi:10.1029/2006JD007847.

Raghoebarsing, A. A., et al. (2005), Methanotrophic symbionts provide carbon for photosynthesis in peat bogs, *Nature*, 436, 1153–1156, doi:10.1038/nature03802.

Roulet, N. T., A. Jano, C. A. Kelley, L. F. Klinger, T. R. Moore, R. Protz, J. A. Ritter, and W. R. Rouse (1994), Role of the Hudson Bay Lowland as a source of atmospheric methane, *J. Geophys. Res.*, 99(D1), 1439–1454, doi:10.1029/93JD00261.

Sebacher, D. I., R. C. Hariss, K. B. Bartlett, S. M. Sebacher, and S. S. Grice (1986), Atmospheric methane sources: Alaskan tundra bogs, and alpine fen and subarctic boreal marsh, *Tellus, Ser. B*, 38, 1–10, doi:10.1111/j.1600-0889.1986.tb00083.x.

Seiler, W. (1984), Contribution of biological processes to the global budget of CH₄ in the atmosphere, in *Current Perspectives in Microbial Ecology*, edited by M. J. Klug and C. A. Reddy, pp. 468–477, Am. Soc. for Microbiol., Washington, D. C.

Twenhofel, W. H. (1926), *Treatise on Sedimentation*, Williams and Wilkins, Baltimore, Md.

Twenhofel, W. H. (1951), *Principles of Sedimentation*, 78 pp., McGraw Hill, New York.

van Beek, L. P. H. (2007), PCR-GLOBWB model description, in *Integration of GFS Data with PCR-GLOBWB using FEWS*, report, WL-Delft Hydraul., Delft, Netherlands. (Available at http://vanbeek.geo.uu.nl/suppinfo/vanbeekbierkens2009.pdf)

van der Molen, M. K., J. van Huissteden, F. J. W. Parmentier, A. M. R. Petrescu, A. J. Dolman, T. C. Maximov, A. V. Kononov, S. V. Karsanaev, and D. A. Suzdalov, (2007), The growing season greenhouse gas balance of a continental tundra site in the Indigirka lowlands, NE Siberia, *Biogeosciences*, 4, 985–1003.

van Huissteden, J., T. C. Maximov, and A. J. Dolman (2005), High CH₄ flux from an arctic floodplain (Indigirka lowlands, eastern Siberia), *J. Geophys. Res.*, 110, G02002, doi:10.1029/2005JG000010.

van Huissteden, J., M. Van den Bos, and I. Martcorena-Alvarez (2006), Modelling the effect of water-table management on CO₂ and CH₄ fluxes from peat soils, Neth. J. Geosci., 85, 3–18.

van Huissteden, J., A. M. R. Petrescu, D. M. D. Hendriks, and K. T. Rebel (2009), Sensitivity analysis of a wetland CH₄ emission model based on temperate and arctic wetland sites, *Biogeosciences*, 6, 3035–3051.

Verdin, K. L. (1997), A system for topologically coding global drainage basins and stream networks, paper presented at the 17th Annual ESRI Users Conference, San Diego, Calif., 8–11 July.

Walter, B. P., and M. Heimann (2000), A process-based, climate-sensitive model to derive CH₄ emissions from natural wetlands: Application to five wetland sites, sensitivity to model parameters, and climate, *Global Biogeochem. Cycles*, 14, 745–765, doi:10.1029/1999GB001204.

Walter, B. M., M. Heimann, and E. Matthews (2001), Modeling modern methane emissions from natural wetlands: 1. Model description and results, *J. Geophys. Res.*, 106(D24), 34,189–34,206, doi:10.1029/2001JD900165.

Walter, K. M., S. A. Zimov, J. P. Chanton, D. Verbyla, and F. S. Chapin III (2006), Methane bubbling from Siberia thaw lakes as a positive feedback to climate warming, *Nature*, 443, doi:10.1038/nature05040.

Walter, K. M., L. C. Smith, and F. S. Chapin III (2007), Methane bubbles from northern lakes: Present and future contributions to the global methane budget, *Philos. Trans. R. Soc. A*, 365, 1657–1676, doi:10.1098/rsta.2007.2036.

Wania, R., I. Ross, and I. C. Prentice (2010), Implementation and evaluation of a new methane model within a dynamic global vegetation model: LPJ-WHyMe v1.3, *Geosci. Model Dev. Discuss.*, 3, 1–59.

Whalen, S. C., and W. S. Reeburgh (1988), A methane flux time series for tundra environments, *Global Biogeochem. Cycles*, 2, 399–409, doi:10.1029/GB002i004p00399.

World Meteorological Organization (1986), *Atmospheric Ozone 1985*, Rep. 16, vol. 1, 478 pp., World Meteorol. Org., Geneva.

Worthy, D. E. J., I. Levin, F. Hopper, M. K. Ernst, and N. B. A. Trivett (2000), Evidence for a link between climate and northern wetland methane emissions, *J. Geophys. Res.*, 105(D3), 4031–4038, doi:10.1029/1999JD901100.

Zimov, S. A., E. A. G. Schuur, and F. S. Chapin III (2006), Permafrost and the global carbon budget, *Science*, 312, 1612–1613.

C. A. R. Corradi, Laboratory of Forest Ecology, Department of Forest Environment and Resources, University of Tuscia of Viterbo, I-01100 Viterbo, Italy.

A. J. Dolman, F. J. W. Parmentier, and J. van Huissteden, Department of Hydrology and Geo-Environmental Sciences, Faculty of Earth and Life Sciences, VU University Amsterdam, De Boelelaan 1085, NL-1081 HV, Amsterdam, Netherlands.

A. M. R. Petrescu, Climate Change Unit, Institute for Environment and Sustainability, DG Joint Research Centre, European Commission, TP290, Via Enrico Fermi 2749, I-21027 Ispra (VA), Italy. (roxana.petrescu@jrc.ec.europa.eu)

C. Prigent, Département de Radioastronomie Millimétrique, Observatoire de Paris, 61 Ave. de l'Observatoire, F-75014 Paris, France.

T. Sachs, Helmholtz Centre Potsdam, German Research Centre for Geosciences, Telegrafenberg B325, D-14473 Potsdam, Germany.

L. P. H. van Beek, Department of Physical Geography, Utrecht University, Heidelberglaan 2, NL-3508 TC, Utrecht, Netherlands.